Desalination and Water Treatment
www.deswater.com

21 (2010) 23–32
September

1944-3994/1944-3986
doi: 10.5004/dwt.2010.1162

Reverse osmosis modeling with the orthogonal collocation on finite element method

Belkacem Absar[a]*, Sid El Mahi Lamine Kadi[a], Omar Belhamiti[b]

[a]*Laboratoire d'Energie-Environnement et Développement Durable, Université de Mostaganem, 27000 Mostaganem, Algérie*
Tel. +213770658646; Fax. +21345333395; email: abbelkacem@univ-mosta.dz; belkacem.absar@laposte.net
[b]*Laboratoire de Mathématiques Pures et Appliquées, Université de Mostaganem, 27000 Mostaganem, Algérie*

Received 30 March 2010; accepted 17 March 2010

ABSTRACT

A mathematical model was used to predict the performance of hollow fiber reverse osmosis membrane. The model is based on the solution-diffusion mass transfer model and takes into account the effect of the flow pattern of the permeate in the membrane. According to the flow direction inside the membrane, two types of flow can be distinguished: the co-current and counter-current flow pattern. Several studies underlined the effectiveness of the counter-current flow pattern [1]. However, no study was carried out to demonstrate this assumption. This work aims to answer clearly the question of the choice of the flow type. The parameters used in this work are the overall recovery, the average concentration of the obtained product and the final concentration of the feed rate in the closed loop processes. The resolution of the mathematical model developed for the counter-current flow pattern is subjected to the split boundary value problem. To solve this problem, a robust and efficient procedure based on orthogonal collocation on finite element method was used. Experimental data were used to verify the proposed mathematical model and accomplish the comparative study between the two flow types. The results obtained show clearly the better efficiency of the counter-current flow pattern especially in the concentrating process.

Keywords: Reverse osmosis; Co-current; Counter-current; Orthogonal collocation; Finite elements

1. Introduction

In the literature, many research works refer to the utilization of the reverse osmosis as a technique to separate dissolved matter. It is a method of separation and concentration in liquid phase. This process is applied to purify water for laboratory use and is very promising as a pre-concentration technique in trace and environmental analysis. The major advantage of this process is that it can be performed at ambient temperature and does not require any energy for initial heating of the feed as it is the case of the distillation processes, and no phase change is involved [2].

The process consists in passing aqueous solution under pressure through an appropriate membrane and withdrawing the membrane permeate at atmospheric pressure and ambient temperature. The product obtained is enriched in one of the mixture components. The others components are recovered in the retentate with higher concentration in the high-pressure side of the membrane. Many mathematical models were developed to describe the behavior of this process [2–7]. These models also predict the performances of reverse osmosis units for a better running. However,

*Corresponding author

the majority of these studies considers only co-current flow and do not take account counter-current flow.

This study proposes to use a simple and effective mathematical model developed for the hollow-fiber membrane modules. It takes account of the flow direction in the feed and the permeate side of the membrane. It allows the simultaneous study of the co-current and the counter-current flow patterns.

Two main purposes of this work are: to formulate a simplified model to predict the performance of RO unit with co-current and counter-current flow, and to compare the results for the two types of flow. The ability to study the two types of flow allows to emphasize the importance and the effectiveness of the counter-current in terms of overall system recovery and purity rate.

The numerical resolution of the proposed mathematical model is carried out using the orthogonal collocation on the finite element method. This technique of resolution is powerful in the split boundary value problem in the mathematical model for a counter-current flow. This work is organized as follows:

Section 2 gives the fundamental equations that describe the transport phenomena in reverse osmosis using the solution-diffusion model and the material balance equations for the hollow fiber module.

Section 3 presents the resolution method used to resolve the mathematical model described above with a brief review of the orthogonal collocation on the finite element method.

In sections 4 and 5, the results obtained by simulation are compared with those of the literature, to highlight the effect of the flow direction on the overall system recovery.

2. Mathematical model

Many mechanistic and mathematical models have been proposed to describe reverse osmosis membranes. Models that adequately describe the performance of reverse osmosis membranes are very important since these are needed in the design of reverse osmosis units.

Among these, the solution-diffusion model is the most used. It is based on the diffusion of the solvent and the solute trough the membrane. This model assumes that both solute and solvent dissolve at the membrane surface and then diffuse across it. The solute and solvent diffusion are separate processes resulting from concentration and pressure differences across the membrane.

2.1. Transport equations

The mass transfer model employed in this study is the solution-diffusion model. The solvent mass flux, J_w, which is generally water, can be expressed by Fick's law. It depends on transmembrane pressure ΔP and the osmotic pressure of the solution on the feed and the permeate side of the membrane [8–9]:

$$J_w = A_w(\Delta P - \Delta\pi), \tag{1}$$

A_w is the water permeability constant,
$\Delta\pi$ represents the difference in osmotic pressure on both sides of the membrane. It is expressed as:

$$\Delta\pi = \pi_F - \pi_P, \tag{2}$$

where the subscripts F refers to the feed side and the subscript P to the permeate side.

For moderate solute concentration, the osmotic pressure is approximately a linear function of solute concentrations [10,11]:

$$\pi = \kappa\, C, \tag{3}$$

where κ is a proportionality coefficient [10–12]. By substituting Eq. (3) into Eq. (1) we obtain:

$$J_w = A_w(\Delta P - \kappa\,\Delta C), \tag{4}$$

where ΔC is the difference in solute concentration across the membrane, expressed as:

$$\Delta C = C_F - C_P, \tag{5}$$

where C_F and C_P are the concentration in the feed and the permeate side, respectively.

The volumetric flow rate can be expressed as:

$$Q_w = \frac{J_w Sa}{\rho_w}, \tag{6}$$

where Sa is the membrane surface area and ρ_w is the water density.

For the solute flux, it is assumed that the chemical potential difference due to pressure is negligible and so the driving force is almost entirely due to concentration differences. From Fick's law, the solute mass flux is:

$$J_s = B_s(\Delta C), \tag{7}$$

where B_s is the solute permeability coefficient which is a function of the solute composition and membrane structure.

The solute mass flow rate is expressed as:

$$\dot{Q}_s = J_s Sa = B_s Sa(C_F - C_P). \tag{8}$$

The membrane rejection rate is defined as the fraction of solute present in the solution which is stopped by the membrane:

$$T_{\mathrm{R}} = \frac{C_{\mathrm{F}} - C_{\mathrm{P}}}{C_{\mathrm{F}}} = 1 - \frac{C_{\mathrm{P}}}{C_{\mathrm{F}}}. \tag{9}$$

Using the relations for solvent and solute flux, the solute rejection rate for the solution-diffusion model can be expressed as:

$$\frac{1}{T_{\mathrm{R}}} = 1 + \frac{B_{\mathrm{s}}\rho_{\mathrm{w}}}{A_{\mathrm{w}}}\left(\frac{1}{\Delta P - \Delta\pi}\right). \tag{10}$$

Equation (10) shows that at high pressures, the rejection rate approaches unity.

Other parameters can be defined to determine the performances of a reverse osmosis system. The water recovery is a production term which relates permeate and feed flows. This factor is a function of time. It can be expressed as:

$$WR_{\mathrm{t}} = \frac{Q_{\mathrm{P}}}{Q_{\mathrm{F}}}. \tag{11}$$

For the overall system, recovery can be defined as the permeate production divided by the initial feed volume. This is used in the closed loop batch concentrating mode. This time independent term can be expressed by:

$$WR_{\mathrm{ov}} = \frac{V_{\mathrm{P}}}{V_{\mathrm{F}}^{0}}. \tag{12}$$

2.2. Hollow fiber membrane mathematical model

The most widely used membrane modules are the spiral-wound, and hollow fiber elements. Membranes of hollow fibers are contained in a shell and the hole constitutes the module. The feed can be introduced either on the shell side or on the fiber side. Permeate is usually withdrawn in a co-current or counter-current manner, with the latter being generally more effective [1]. The flow patterns for both the co- and counter-current flows are illustrated in Fig. 1.

2.2.1. Co-current flow pattern

In this flow pattern, the permeate and the feed in the fiber side and the shell, respectively, flow co-currently. According to the solution-diffusion model, the rate of permeate in an elemental section length Δx for water is Q_{pw}:

$$Q_{\mathrm{pw}} = \frac{A_{\mathrm{w}}}{\rho_{\mathrm{w}}}(\pi D_{\mathrm{m}}\Delta x)\,(\Delta P - \kappa(C_{\mathrm{F}} - C_{\mathrm{P}})), \tag{13}$$

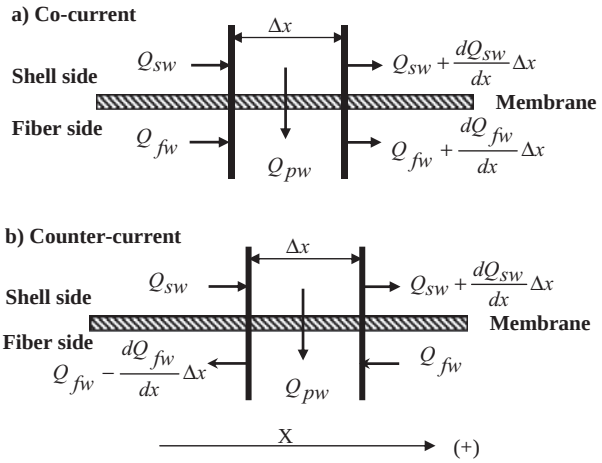

Fig. 1. Flowrate change across section Δx.

where D_{m} is the membrane mean diameter

The material balance for water in the shell side can be written as:

$$Q_{\mathrm{sw}} = \left(Q_{\mathrm{sw}} + \frac{\mathrm{d}Q_{\mathrm{sw}}}{\mathrm{d}x}\Delta x\right) + Q_{\mathrm{pw}}, \tag{14}$$

where Q_{sw} is the water volumetric flow rate in the shell side. The first subscript indicates the shell or the fiber side, and the second subscript indicates the solute or the water.

This equation can be written in the following form:

$$\frac{\mathrm{d}Q_{\mathrm{sw}}}{\mathrm{d}x} = -\frac{Q_{\mathrm{pw}}}{\Delta x}. \tag{15}$$

Substituting Q_{pw} for its expression in Eq. (13) gives:

$$\frac{\mathrm{d}Q_{\mathrm{sw}}}{\mathrm{d}x} = -\frac{A_{\mathrm{w}}}{\rho_{\mathrm{w}}}(\pi D_{\mathrm{m}})\,(\Delta P - \kappa(C_{\mathrm{F}} - C_{\mathrm{P}})), \tag{16}$$

C_{F} can be expressed as:

$$C_{\mathrm{F}} = \frac{\dot{Q}_{\mathrm{ss}}}{Q_{\mathrm{sw}}}, \tag{17}$$

where $\dot{Q}_{\mathrm{ss}}$is the solute mass flow rate in the shell side and $\dot{Q}_{\mathrm{sw}}$ is the volumetric flow rate.

A similar equation is obtained for the solute concentration C_{P} in the permeate flow rate (fiber side):

$$C_{\mathrm{p}} = \frac{\dot{Q}_{\mathrm{fs}}}{Q_{\mathrm{fw}}},$$

where $\dot{Q}_{fs}$ and Q_{fw} are, respectively, the solute mass flow rate and the water volumetric flow rate in the fiber side.

Substituting C_F and C_p for their expressions in Eq. (16) gives:

$$\frac{dQ_{sw}}{dx} = -\frac{A_w}{\rho_w}(\pi D_m)\left(\Delta P - \kappa\left(\frac{\dot{Q}_{ss}}{Q_{sw}} - \frac{\dot{Q}_{fs}}{Q_{fw}}\right)\right). \quad (18)$$

The material balance for water on the fiber side is obtained in the same manner:

$$\frac{dQ_{fw}}{dx} = \frac{A_w}{\rho_w}(\pi D_m)\left(\Delta P - \kappa\left(\frac{\dot{Q}_{ss}}{Q_{sw}} - \frac{\dot{Q}_{fs}}{Q_{fw}}\right)\right). \quad (19)$$

Similarly, the material balance for the solute in the shell side (Fig. 1) can be written as:

$$\dot{Q}_{ss} = \left(\dot{Q}_{ss} + \frac{d\dot{Q}_{ss}}{dx}\Delta x\right) + \dot{Q}_{ps}, \quad (20)$$

where $\dot{Q}_{ss}$ is the solute mass flow rate in the shell side, and $\dot{Q}_{ps}$ the solute mass flow rate across the membrane.

Arranging this equation and substituting $\dot{Q}_{ps}$ for its expression Eq. (8) gives:

$$\frac{d\dot{Q}_{ss}}{dx} = -B_s(\pi D_m)\left(\frac{\dot{Q}_{ss}}{Q_{sw}} - \frac{\dot{Q}_{fs}}{Q_{fw}}\right). \quad (21)$$

A similar equation is obtained for the fiber side:

$$\frac{d\dot{Q}_{fs}}{dx} = B_s(\pi D_m)\left(\frac{\dot{Q}_{ss}}{Q_{sw}} - \frac{\dot{Q}_{fs}}{Q_{fw}}\right). \quad (22)$$

Finally, the mathematical model obtained is composed of a set of four ordinary differential equations. To determine the permeate flow rate at the end of the module, equations (18), (19), (21) and (22) must be integrated simultaneously.

2.2.2. Counter-current flow pattern

In this flow pattern, the permeate and the feed in the fiber side and the shell side flow counter currently.

A similar set of differential equations is obtained for the counter-current flow pattern:

$$\begin{cases} \dfrac{dQ_{sw}}{dx} = -\dfrac{\pi D_m A_w}{\rho_w}\left(\Delta P - \kappa\left(\dfrac{\dot{Q}_{ss}}{Q_{sw}} - \dfrac{\dot{Q}_{fs}}{Q_{fw}}\right)\right) \\ \dfrac{dQ_{fw}}{dx} = -\dfrac{\pi D_m A_w}{\rho_w}\left(\Delta P - \kappa\left(\dfrac{\dot{Q}_{ss}}{Q_{sw}} - \dfrac{\dot{Q}_{fs}}{Q_{fw}}\right)\right) \\ \dfrac{d\dot{Q}_{ss}}{dx} = -\pi D_m B_s\left(\dfrac{\dot{Q}_{ss}}{Q_{sw}} - \dfrac{\dot{Q}_{fs}}{Q_{fw}}\right) \\ \dfrac{d\dot{Q}_{fs}}{dx} = -\pi D_m B_s\left(\dfrac{\dot{Q}_{ss}}{Q_{sw}} - \dfrac{\dot{Q}_{fs}}{Q_{fw}}\right) \end{cases}$$

These equations constitute the mathematical model for a counter-current flow pattern.

The models presented in this study describe ideal mass transfer and do not take account of the concentration polarization. Concentration polarization describes the accumulation of rejected solute at the surface of the membrane, and can be minimized by increasing the feed velocity [10].

2.3. Process modeling

Fig. 2 shows a schematic of a process operating in continuous mode. It consists of a feed tank, a product tank and the membrane module. The retentate is recycled to the feed tank and the permeate is collected separately in the product tank. This process is essentially used in a concentrating system [13–15].

The material balance equation applied to product tank yields:

$$Q_P\, C_P = \frac{d\left(V_p\, C_{Pavg}\right)}{dt}, \quad (23)$$

where C_{Pavg} is the average concentration of the obtained product and V_P its volume after a defined operating time.

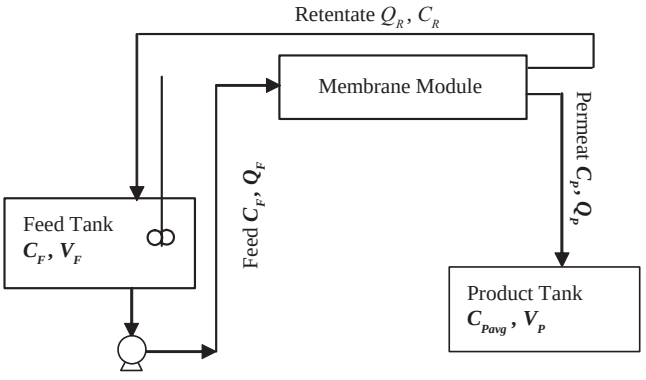

Fig. 2. Schematic of reverse osmosis system.

Development of this equation gives:

$$Q_P C_P = V_p \frac{dC_{pavg}}{dt} + C_{Pavg} \frac{dV_p}{dt}. \quad (24)$$

At the initial conditions: $t = 0$, $V_p = 0$, $C_{Pavg} = C_P = 0$. The change in the volume of product corresponds to the production rate of the membrane:

$$\frac{dV_p}{dt} = Q_P. \quad (25)$$

Substitution into Eq. (24) gives:

$$\frac{dC_{pavg}}{dt} = \frac{Q_P(C_P - C_{pavg})}{V_p}. \quad (26)$$

The material balance on the membrane module yields:

$$Q_F C_F = Q_P C_P + Q_R C_R. \quad (27)$$

Similar material balance equation around the feed tank can be obtained:

$$Q_R C_R - Q_F C_F = \frac{d(V_{Ft} C_{Ft})}{dt}. \quad (28)$$

Developing this equation yields:

$$-Q_P C_P = V_{Ft} \frac{dC_{Ft}}{dt} + C_{Ft} \frac{dV_{Ft}}{dt}, \quad (29)$$

where V_{Ft} is the volume in the feed tank at a time t, with a concentration inside the tank as C_{Ft}. The feed tank is assumed well mixed. Thus the concentration of the feed at the membrane module is equal at the concentration in the feed tank:

$$V_{Ft} = V_F \quad (30)$$

and

$$C_{Ft} = C_F. \quad (31)$$

The change volume in the feed tank with time corresponds to the production rate:

$$-\frac{dV_F}{dt} = Q_P. \quad (32)$$

Integrating this equation at the initial conditions: $t = 0$, $V_F = V_F^0$

$$V_F = V_F^0 - Q_P t. \quad (33)$$

Substituting these expressions in Eq. (29) yields:

$$\frac{dC_F}{dt} = \frac{Q_P(C_F - C_P)}{(V_F^0 - Q_P t)}. \quad (34)$$

One parameter of interest is the overall recovery, WR_{ov}, which can be obtained from Eq. (12).

Since the operating system is closed, the mass conservation implies that the mass of the solute in the feed tank at initial time, is equal to the sum of the various process streams and tanks at any instant of time. So:

$$V_P = \frac{V_F^0(C_F - C_F^0)}{C_F - C_{Pavg}}. \quad (35)$$

Substituting V_P for its expression in Eq. (26) gives:

$$\frac{dC_{pavg}}{dt} = \frac{Q_P(C_P - C_{pavg})}{V_F^0(C_F - C_F^0)}(C_F - C_{Pavg}). \quad (36)$$

Equations (34) and (36) are the result of material balances on the feed tank, product tank and the membranes module. The resolution of this set of two ordinary differential equations requires the values of C_P and Q_P. These values are obtained by integrating the set of ordinary differential equations developed above for co-current or counter-current flow.

Solution of Eq. (34) provides the concentration feed as a function of the operating time. Thus, the solute rejection rate can be determined at any time.

Solution of Eq. (36) provides the average concentration of the solute in product tank and so the water volume by using equation (35). Eq. (12) gives the value of the water overall recovery.

3. Methods of resolution

The method of orthogonal collocation as described by Villadsen and Michelsen [16], can lead to the numerical resolution of many problems. However, it does not prove very effective for certain cases where the solution is very irregular. To avoid this problem, it is necessary to take a very great order of approximation. It is a disadvantage which limits the application fields of this technique. This is the reason why the orthogonal collocation method is combined with the finite element method.

In this work, the orthogonal collocation on the finite element method as a numerical method to solve the boundary value problems is chosen due to its efficiency and robustness.

Tessendorf et al. [17] have used the orthogonal collocation on finite element method to solve a set of nonlinear coupled differential equations. Gauss method

was used to solve the nonlinear algebraic equations system.

In our approach [18], an iterative technique was developed to uncouple and linearize the system of the differential equations. The nonlinear coupled system is thus transformed to an uncoupled linear system. This linearization allows more stability. The numerical resolution of the proposed mathematical model using this procedure has led to results with high precision (check of material balance with high precision).

Our technique consists in giving an initial profile of solution for each equation which verifies the boundary conditions, $y_1^{(1)}, y_2^{(1)}, y_3^{(1)}, y_4^{(1)}$. The iterative procedure can be written as:

$$\begin{cases} \dfrac{dy_1^{(k+1)}}{dx} = f_1\left(x, y_1^{(k)}, y_2^{(k)}, y_3^{(k)}, y_4^{(k)}\right) \\ \dfrac{dy_2^{(k+1)}}{dx} = f_2\left(x, y_1^{(k+1)}, y_2^{(k)}, y_3^{(k)}, y_4^{(k)}\right) \\ \dfrac{dy_3^{(k+1)}}{dx} = f_3\left(x, y_1^{(k+1)}, y_2^{(k+1)}, y_3^{(k)}, y_4^{(k)}\right) \\ \dfrac{dy_4^{(k+1)}}{dx} = f_4\left(x, y_1^{(k+1)}, y_2^{(k+1)}, y_3^{(k+1)}, y_4^{(k)}\right) \end{cases} \tag{37}$$

where $y_i^{(k+1)}$ and $y_i^{(k)}$ are the approximations of the solution y_i at the current and the preceding iteration, respectively.

At each iteration, the orthogonal collocation on the finite element method is applied to each linear differential equation. Thereafter we can calculate the uncoupling error by using the following formula:

$$\begin{aligned} \text{Error} = \text{Max}\Big(& \left\| y_1^{(k+1)} - y_1^{(k)} \right\|_2, \\ & \left\| y_2^{(k+1)} - y_2^{(k)} \right\|_2, \left\| y_3^{(k+1)} - y_3^{(k)} \right\|_2, \\ & \left\| y_4^{(k+1)} - y_4^{(k)} \right\|_2 \Big), \end{aligned} \tag{38}$$

where $\| . \|_2$ is the Euclidean norm.

This procedure gives the solution of the problem, when the error is under a given small epsilon ($\varepsilon \sim$ 1.0e-10).

To explain the procedure, we consider the following differential equation in the domain Ω:

$$y'(x) + a(x)\,y(x) = f(x). \tag{39}$$

Figure 3 shows the discretizing of the domain Ω. It is divided into n elements. After that, the orthogonal collocation is applied in each element $\left(\Omega^{(i)}\right)_{i=1..n}$.

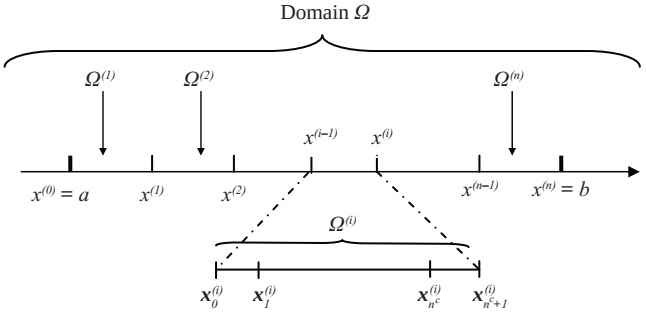

Fig. 3. Finite element collocation discretizing.

For the choice of the internal collocation points, we use the roots of the Jacobi orthogonal polynomials of degree N defined in the domain [0 1].

$$J_N^{(\alpha,\beta)}(x) = \sum_{i=0}^{N} (-1)^{N-i} \gamma_{N,i} x^i$$

where

$$\gamma_{N,i} = \frac{N-i+1}{i} \frac{N+i+\alpha+\beta}{i+\beta} \gamma_{N,i-1}.$$

With $\gamma_{N,0} = 1$.

α and β are the polynomial characteristic parameters

The elementary solution of Eq. (39) in the ith element is given by:

$$y^{(i)}(x) = \sum_{j=0}^{n^c+1} y_j^{(i)}\, l_j(x), \tag{40}$$

where n^c is the number of internal collocation points and $l_j(x)$ is the jth degree Lagrange polynomials.

Substitution of Eq. (40) into Eq. (39) generates residual:

$$R(x) = \frac{dy^{(i)}(x)}{dx} + a(x)\, y^{(i)}(x) - f(x). \tag{41}$$

The weighted functions ψ_j are then used to reduce the residual to a minimum value, for $j=0..n^c+1$:

$$\psi_j(x) = \begin{cases} 1 & \text{for } x = x_j^c \\ 0 & \text{for } x \neq x_j^c \end{cases} \tag{42}$$

and

$$\int_{x_0^{(i)}}^{x_{n^c+1}^{(i)}} R(x)\ \ \psi_j(x)\, dx = 0. \tag{43}$$

Consequently:

$$R(x_j^c) = 0. \quad (44)$$

Substituting the expressions of $\frac{dy^{(i)}}{dx}\left(x_j^c\right)$ and $y^{(i)}\left(x_j^c\right)$ in Eq. (44) leads to a linear system with (n^c+2) equations and (n^c+2) unknowns:

$$M^{(i)}y^{(i)} = b^{(i)}, \quad (45)$$

$M^{(i)}$ and $b^{(i)}$ are the elementary matrix and its second member in the ith element $\Omega^{(i)}$

By applying the same procedure to each element $\left(\Omega^{(i)}\right)_{i=1..n}$, n systems of algebraic linear equations are obtained. These linear systems are assembled into a global system expressed as follows:

$$M^G\, y \;=\; b^G \quad (46)$$

$M^G$and $b^G$are the global matrix and its second member. The vector y represents the global solution of Eq. (39) on Ω.

4. Model verification

The model presented in Section 2, was verified with experimental data from literature [13–15]. The membrane specifications and the operating parameters are given in Table 1.

5. Results and discussion

Two simulations were run using the preceding data. In the first simulation, the two types of flow pattern were studied. This makes possible the comparison of the two modules performances. The module operating in counter-current can however operate longer than the co-current.

In the second simulation, only the counter-current module was studied. The results obtained show that the time of separation can be prolonged thus offering better performances.

Table 1
Parameters value

Parameter	Values
Initial feed concentration (C_F^0)	2 0 kg/m^3
Initial volume in the feed tank (V_F^0)	0.15 m^3
Membrane surface area (S_a)	0.181 m^2
Water density (ρ_w)	1000 kg/m^3
Transmembrane pressure (ΔP)	4.02×10^{13} kg/m h^2
Proportionality coefficient (α)	1.02×10^{12} m^2/h^2
Water permeability constant (A_w)	4.20×10^{-13} h/m
Solute permeability coefficient (B_s)	1.12×10^{-4} m/h

5.1. Co- and counter-current comparative study

For the first simulation, the operating time reached is about 145.5 h. The co-current module cannot operate beyond this time. The concentration in the permeate becomes so significant and consequently the osmotic pressure, that the transmembrane pressure cannot overcome it.

The results obtained for both the co- and the counter-current flow pattern are given in Table 2. Fig. 4 shows the simulation results of the feed concentration with time for the co- and counter-current flow pattern.

The two curves are superimposed and the behavior is similar in both cases. As shown, the feed concentration initially increases linearly with time, then becomes exponential to reach a value of 38.916 kg/m^2 after 145.5 h.

Fig. 5 shows the concentration variation of the permeate and the product with time for the both modules. Either the permeate concentration or the product concentration have a similar behavior in the co and counter-current flow pattern. Initially, the permeate concentration increases gradually, then the variation becomes more important with time and attains a value of 2.810 kg/m^2 after 145.5 h. The product concentration is less significant because of the dilution effect in the product tank.

The comparison of the overall recovery for the co- and counter-current, shows that this parameter behaves in the same manner and reaches after the operating time a value of 95.766% in the co-courant flow, and a value of 95.767% in the counter-courant flow (Fig. 6). To discuss the differences between the two types of flow pattern, an error term was used and which consists in computing the difference between the feed concentration in both cases, then plotting this error term versus time. The results obtained show that the error is very close to zero. However, after 140 h, this value increases abruptly. This is explained by the fact that beyond this time, the improvement of the value of the feed concentration in the case of the counter-current

Table 2
Comparative results for co- and counter-current

Parameter	Co-current	Counter-current
Feed concentration (kg/m^3)	38.916	38.920
Average product concentration (kg/m^3)	0.368	0.368
Overall recovery (%)	95.766	95.767

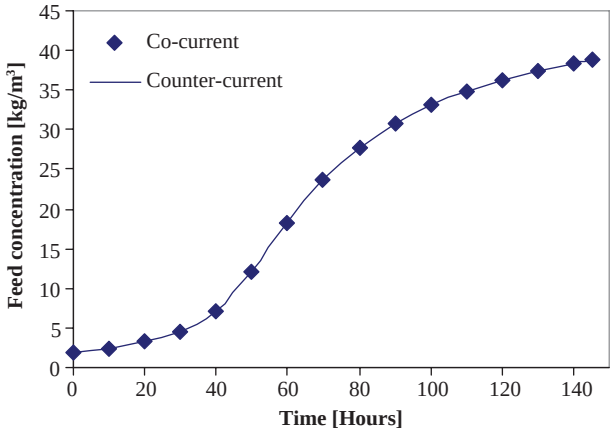

Fig. 4. Feed concentration vs. time in the co- and counter-current flow pattern.

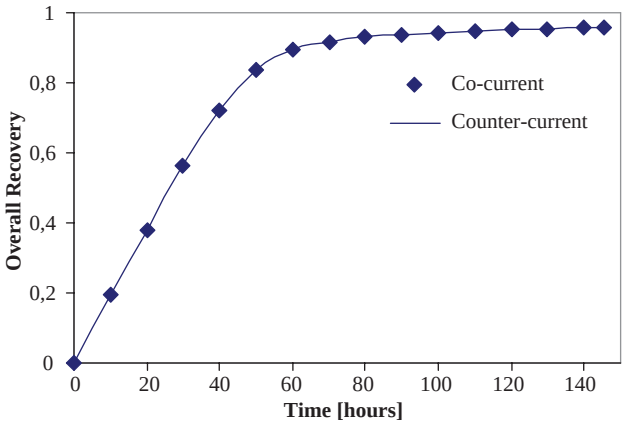

Fig. 6. Overall recovery vs. time in the co- and counter-current flow pattern.

flow is more significant than that of the co-current flow, see Fig. 7.

5.2. Counter-current simulation

The module with a co-current flow can operate only during 145.5 h. The counter-current can operate longer. In the second simulation, only the counter-current was performed. The time of separation reaches a value of 152.5 h which represents an additional time of 7 h of supplementary separation compared to the first simulation (Fig. 8). The results obtained are given in Table 3.

As shown in Table 3, the prolongation of the operating time enables to improve separation by increasing the overall recovery. However the concentration of the product increases. The feed concentration reaches values larger than those obtained in the first simulation. This is due to the recycling of the retentate which becomes more and more concentrated. The use of the counter-current flow pattern in the reverse osmosis system appears more interesting in the processes of concentration.

6. Conclusion

The purpose of this work was to develop a mathematical model for reverse osmosis, to propose an efficient and robust numerical solution procedure for the resulting set of differential model equations, and to highlight the importance and efficiency of the counter-current flow pattern. The mathematical model developed in this study takes into account two different flow patterns: the co-current and the counter-current pattern. The determination of the permeate flux through the membrane was based on the solution-diffusion model. The solution procedure to solve the differential model combines the

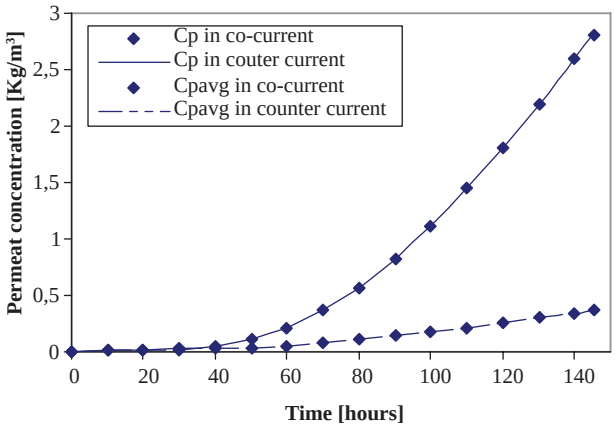

Fig. 5. Product and permeate concentration in the co- and counter-current flow pattern.

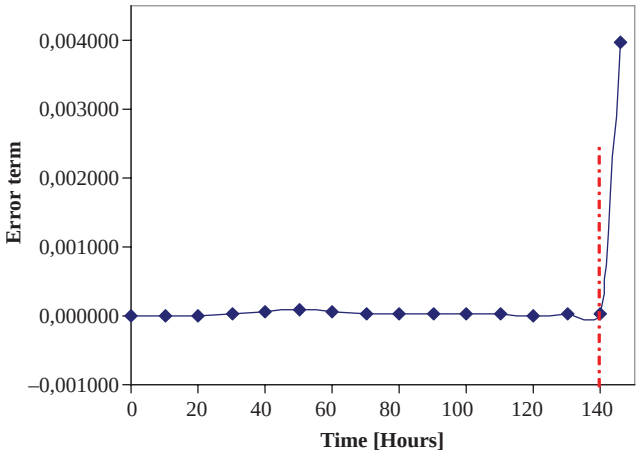

Fig. 7. Difference between the feed concentration in the co- and counter-current flow pattern vs. time.

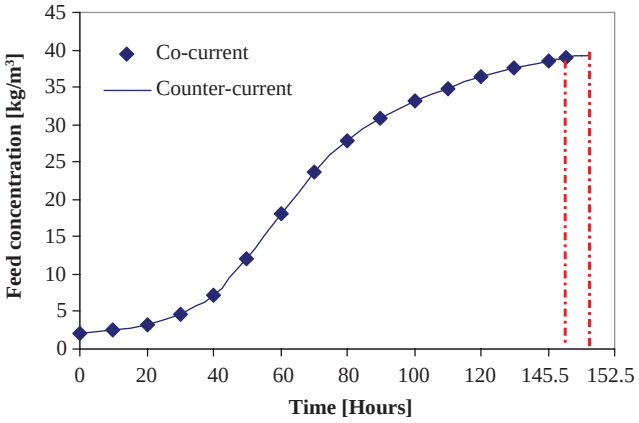

Fig. 8. Feed concentration in the first and second simulation vs. time

orthogonal collocation and the finite element method to have higher precision. The overall recovery, the feed concentration and the product concentration can be affected by the flow pattern. It was shown that the counter-current flow pattern is more efficient than the co-current one. The overall recovery in the counter-current flow pattern is more significant. However, the improvement observed in the overall recovery, is obtained to the detriment of the quality of the product obtained since its concentration also increases. Thus, the use of the counter-current mode appears more interesting in the processes of concentration. Longer operating times result in higher product concentration.

Symbols

A_w	water permeability constant, h/m,
B_s	solute permeability coefficient, m/h,
$b^{(i)}$	second member of the elementary matrix in the ith element $\Omega^{(i)}$,
b^G	second member of the global matrix,
C	concentration, kg/m^3,
D_m	mean diameter, m,
J_s	solute flux, kg/m^2 h,
J_w	solvent flux, kg/m^2 h,
J_N	Jacobi polynomial of degree N,
$l_j(x)$	Lagrangian interpolation polynomial,
$M^{(i)}$	elementary matrix in the ith element $\Omega^{(i)}$,
M^G	global matrix in the domain Ω,
n^c	number of internal collocation points,
ΔP	transmembrane pressure, kg/m h^2,
Q	volumetric flow rate, m^3/ h,
$\dot{Q}$	mass flow rate, kg/ h,
$R(x)$	residual,
Sa	membrane surface, m^2,
t	time, h,
T_1R	solute rejection,
V	volume, m^3,
WR_t	water recovery,
WR_{ov}	overall recovery,
Δx	elemental section length, m,
$y_i^{(k)}$	approximation of the solution y_i at the kth iteration.

Greek letters

α	polynomial characteristic parameter
β	polynomial characteristic parameters
κ	proportionality coefficient, m^2/h^2,
$\Delta\pi$	osmotic pressure difference, kg/m h^2,
ρ_w	water density, kg/m^3.

Subscripts

F	feed side,
f	fiber side,
P	permeate side,
$pavg$	product average concentration,
R	retentate,
s	shell side,
w	water.

Table 3
Results for counter-current flow simulation

Parameter	Results
Operating time (h)	152.5
Feed concentration (kg/m^3)	39.475
Average product concentration (kg/m^3)	0.399
Overall recovery (%)	95.903

References

[1] J. Marriott and E. Sørensen, Chem. Eng. Sci., 58 (2003) 4975–4990.
[2] A.S. Kahdim, S. Ismail and A.A. Jassim. Desalination, 158 (2003) 323–329.
[3] J. Marriott, E. Sørensen and I.D.L. Bogle, Comput. Chem. Eng. 25 (2001) 693–700.
[4] D.F. Fletcher and D.E. Wiley, J. Membr. Sci., 245 (2004) 175–181.
[5] A. Idris, A.F. Ismail, S.J. Shilton, R. Roslina and M. Musa, Sep. Purif. Technol. 29 (2002) 217–227.
[6] M.G. Marcovecchio, P.A. Aguirre and N.J. Scenna, Desalination, 184 (2005) 259–271.
[7] D.E. Wiley and D.F. Fletcher, Desalination, 145 (2002) 183–186.
[8] N.M. Al-Bastaki and A. Abbas, Desalination, 132 (2000) 181–187.
[9] N.M. Al-Bastaki and A. Abbas, Desalination, 126 (1999) 33–39.
[10] N.M. Al-Bastaki and A. Abbas, Chem, Eng, Process,, 43 (2004) 555–558.

[11] S. Senthilmurugan, A. Ahluwalia and S.K. Gupta, Desalination, 173 (2005) 269–286.
[12] A. Abbas, Desalination, 44 (2005) 999–1004.
[13] C.S. Slater, J.M. Zielinski, R.G. Wendel and C.G. Uchrin, Desalination, 52 (1985) 267–284.
[14] C.S. Slater and C.A. Books, Sep, Sci, Technol, 27 (1992) 1361–1388.
[15] K. Jamal, M.A. Khan and M. Kamil, Desalination, 160 (2004) 29–42.
[16] J. Villadson and M.L. Michelson, Solution of Differential Equations Models by Polynomial Approximation, New Jersey, Prentice Hall, 1978.
[17] S. Tessendorf, R. Gani and M.L. Michelson, Chem. Eng. Sci., 54 (1999) 943–955.
[18] O. Belhamiti, Implémentation de la Méthode de Collocation Orthogonale sur les Eléments Finis: Application sur les Techniques de Séparation Membranaire, Magister Thesis, 2003.